Structure and DNA Binding Activity of Analogues of 1,5-Bis(4-amidinophenoxy)pentane (Pentamidine)

Michael Cory,†,* Richard R. Tidwell, and Terri A. Fairley†

Division of Organic Chemistry, Burroughs Wellcome Co., Research Triangle Park, North Carolina 27709, and Division of Biological Chemistry and Cell Biology, Department of Pathology, School of Medicine, University of North Carolina, Chapel Hill, North Carolina 27599. *Received February 15, 1991*

The DNA binding properties of a series of 39 bisbenzamidines related to the clinically used antipneumocystis drug pentamidine (1) were studied. Changes in the thermal denaturation temperature of calf thymus DNA (ΔT_m) showed that all the compounds have significant affinity for DNA. A comparison of ΔT_ms for the series with ΔT_ms of base-pair-specific DNA-binding compounds, using homopolymers poly(dA)·poly(dT) and poly(dG-dC)·poly(dG-dC), indicated that the compounds show moderate specificity for AT base pairs. Lack of DNA helix extension, measured by viscometric titration with sonicated calf thymus DNA, indicated that the compounds do not bind to DNA by intercalation. Analogues of 1 with an odd number of methylenes connecting the benzamidine rings had a higher affinity for DNA and homopolymers than analogues with an even number of methylenes. All of the compounds containing an amidino group meta to the linking chain showed lower polynucleotide affinity. These results suggest that the shape of the molecules was important for DNA binding. Molecular modeling studies showed a correlation between the DNA binding and the radius of curvature of molecular mechanics models of the molecules. Monosubstitution on the benzamidine rings or replacement of the amidino group with the cyclic imidazolino group had no influence on the DNA-binding affinity of the compounds. Substitution of NH for the ether oxygen connecting group of 1 had no effect on the DNA binding or base-pair specificity. Methylation of either of the nitrogen atoms of the imidazolino group to provide an analogue of 1 with *N*-methylimidazolino groups decreased DNA affinity considerably. GC vs AT base-pair specificity as measured by ΔT_m does not correlate with the radius of curvature. The experimental and modeling results are consistent with DNA minor-groove binding.

Pentamidine (1), a bisbenzamidine, is effective in the treatment of *Pneumocystic carinii* pneumonia (PCP) in humans and has proven useful in treating AIDS-related PCP.[1,2] In a previous paper,[3] we presented the synthesis and antiinfective activity, against a rat model of PCP, for a series of 33 analogues of 1. The previous paper presented evidence that compounds active against PCP in animals showed weak activity against the enzymes trypsin ($K_i > 10^{-3}$) or thymidylate synthase ($I_{50} = 10^{-3}$–10^{-1}). This effectively ruled out these enzymes as targets of the anti-PCP action for 1 and its analogues.

The relationship of the DNA-binding properties of the compounds with anti-PCP activity also was not definitive. All compounds studied in the previous paper showed some binding to calf thymus DNA, as indicated by a thermal denaturation measurement (ΔT_m), and all of the pentamidine analogues that were not toxic or insoluble were active against PCP in vivo. Further, the DNA-binding properties of 1 and its analogues and the possibility that the DNA-binding properties correlate with the anti-PCP activity of the pentamidine analogues remained to be explored. Later work[4] indicated that these compounds also show significant in vitro activity against *Giardia lamblia*, *Plasmodium falciparum*, and *Leishmania mexicana amazonensis*.[5]

Williamson demonstrated that aromatic amidines such as 1 could bind to DNA.[6] Waring explored the mechanism of action of related bisamidines such as berenil (2), and showed that it could bind in the minor groove of DNA.[7] In 1980, Braithwaite and Baguley[8] used viscometric titration of bacteriophage DNA and a competitive ethidium bromide (3) displacement assay to evaluate the base-pair specificity of a series of bisamidines and quaternary ammonium heterocycles with good antitumor activity. They concluded that these compounds can bind in the minor groove of DNA and show moderate AT base-pair specificity. They found AT/GC specificity ratios between 2 and 15 for bisamidines, but a ratio of greater than 500 for a highly specific AT-binding compound, distamycin A (4).

Recently, Brown and co-workers[9] solved a crystal structure of 2 bound to a double-stranded DNA dodecamer. Compound 2 binds in the minor groove of an AATT sequence in the center of the double-stranded dodecamer sequence GCGCAATTGCGC. DNA footprinting studies show that 1 binds best to sites on DNA that consist of at least five consecutive AT base pairs.[10]

† Burroughs Wellcome Co.

(1) Montgomery, A. B.; Luce, J. M.; Turner, J.; Lin, E. T.; Debs, R. J.; Corkery, K. J.; Brunette, E. N.; Hopewell, P. C. Aerosolised pentamidine as sole therapy for *Pneumocystis carinii* pneumonia in patients with acquired immunodeficiency syndrome. *Lancet* **1987** *ii*, 480–482.
(2) Debs, R. J.; Blumenfeld, W.; Brunette, E. N.; Straubinger, R. M.; Montgomery, A. B.; Lin, E.; Agabian, N.; Papahadjopoulos, D. Successful treatment with aerosolized pentamidine of *Pneumocystis carinii* pneumonia in rats. *Antimicrob. Agents Chemother.* **1987**, *31*, 37–41.
(3) Tidwell, R. R.; Jones, S. K.; Geratz, J. D.; Ohemeng, K. A.; Cory, M.; Hall, J. E. Analogues of 1,5-Bis(4-amidinophenoxy)pentane (Pentamidine) in the Treatment of Experimental *Pneumocystis carinii* Pneumonia. *J. Med. Chem.* **1990**, *33*, 1252–1257.
(4) Bell, C. A.; Cory, M.; Fairley, T. A.; Hall, J. E.; Tidwell, R. R., unpublished results.
(5) Bell, C. A.; Hall, J. E.; Kyle, D. E.; Grogl, M.; Ohemeng, K. A.; Allen, M. A.; Tidwell, R. R. Stucture–Activity Relationships of Analogs of Pentamidine against *Plasmodium falciparum* and *Leishmania mexicana amazonensis*. *Antimicrob. Agents Chemother.* **1990**, *34*, 1381–1386.
(6) Williamson, J. Effects of trypanocides on the fine structure of target organisms. *Pharm. Ther.* **1979**, *7*, 445–512.
(7) Waring, M. Variation of the supercoils in closed circular DNA by binding of antibiotics and drugs: Evidence for molecular models involving intercalation. *J. Mol. Biol.* **1970**, *54*, 247–277.
(8) Braithwaite, A. W.; Baguley, B. C. Existence of an Extended Series of Antitumor Compounds Which Bind to Deoxyribonucleic Acid by Nonintercalative Means. *Biochemistry* **1980**, *19*, 1101–1105.
(9) Brown, D. G.; Sanderson, M. R.; Skelly, J. V.; Jenkins, T. C.; Neidle, S.; Brown, T.; Garman, E.; Stuart, D. I. Abstract International Conference on Drug–DNA Interactions. Cambridge, England, Sept 11, 1989.
(10) Fox, K. R.; Sansom, C. E.; Stevens, M. F. G. Footprinting studies on the sequence-selective binding of pentamidine to DNA. *FEBS Lett.* **1990**, *266*, 150–154.

0022-2623/92/1835-0431$03.00/0

Table I. Structure, DNA-Binding Properties, and Base Pair Specificity of Pentamidine and Its Analogues

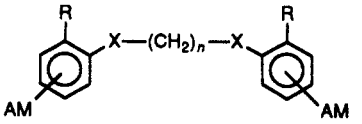

no.	X	n	R	AM	ΔT_m[a] CT	ΔT_m[a] AT	ΔT_m[a] GC	normalized to ethidium bromide: AT	GC	ratio AT/GC
2										
3					12.4 (0.6)	9.9 (1.3)	5.3 (0.7)	1.0	1.0	1.0
4					11.5 (0.7)	30.5 (0.6)	1.9 (0.4)	3.1	0.4	8.6
5					19.0 (1.8)	46.6 (0.1)	1.1 (0.0)	4.7	0.2	22.7
6					14.1 (1.1)	32.4 (0.4)	2.5 (0.3)	3.3	0.5	6.9
7					21.5 (0.8)	42.0 (3.7)	6.9 (0.7)	4.2	1.3	3.3
8	O	2		amidino	5.4 (0.2)	7.5 (2.6)	1.3 (0.0)	0.8	0.2	3.1
9	O	2	NH_2	amidino	8.8 (0.2)	16.4 (0.9)	3.0 (0.3)	1.7	0.6	2.9
10	O	2	NO_2	amidino	5.6 (0.3)	10.3 (0.2)	1.9 (0.2)	1.0	0.4	2.9
11	NH	2	NH_2	amidino	9.8 (0.5)	16.8 (1.9)	3.0 (0.4)	1.7	0.6	3.0
12	O	3		amidino	14.7 (1.7)	32.0 (0.7)	4.5 (0.2)	3.2	0.8	3.8
13	O	3		*m*-amidino	7.6 (1.1)	8.5 (0.5)	3.0 (0.4)	0.9	0.6	1.5
14	O	3	NH_2	amidino	13.6 (0.1)	32.2 (0.7)	5.2 (0.4)	3.3	1.0	3.3
15	O	3	OMe	imidazolino	12.4 (2.5)	34.3 (0.5)	4.1 (0.9)	3.5	0.8	4.5
16	O	3	OMe	amidino	16.3 (0.1)	38.0 (3.0)	3.4 (0.4)	3.8	0.6	6.0
17	NH	3		amidino	11.6 (0.9)	25.7 (4.5)	3.0 (0.2)	2.6	0.6	4.6
18	NH	3	NH_2	amidino	12.4 (2.1)	25.6 (1.0)	4.8 (0.2)	2.6	0.9	2.9
19	NH	3	NO_2	amidino	12.4 (0.8)	26.6 (1.6)	5.0 (0.6)	2.7	0.9	2.8
20	O	4		1-Me-2-imidazolinyl	7.2 (0.1)	4.1 (0.1)	1.5 (0.4)	0.4	0.3	1.5
21	O	4		imidazolino	12.0 (0.1)	15.6 (0.6)	4.8 (0.0)	1.6	0.9	1.7
22	O	4		amidino	8.3 (2.5)	17.9 (1.6)	3.1 (0.4)	1.8	0.6	3.1
23	O	4		*m*-amidino	8.1 (0.6)	15.2 (1.4)	2.6 (0.2)	1.5	0.5	3.1
24	O	4	Cl	amidino	8.9 (0.6)	20.3 (0.5)	4.2 (0.6)	2.1	0.8	2.6
25	O	4	NH_2	amidino	9.6 (0.3)	19.4 (2.3)	3.7 (1.3)	2.0	0.7	2.8
26	O	4	NO_2	amidino	9.6 (1.3)	14.7 (0.5)	3.5 (0.6)	1.5	0.7	2.2
27	O	4	OMe	amidino	10.2 (0.2)	22.9 (0.9)	1.1 (0.5)	2.3	0.2	11.1
28	NH	4		amidino	10.3 (0.8)	18.7 (2.9)	2.8 (0.2)	1.9	0.5	3.6
29	NH	4	NH_2	amidino	10.5 (0.7)	13.2 (0.6)	4.6 (0.4)	1.3	0.9	1.5
30	O	5		1-Me-2-imidazolinyl	5.6 (1.9)	10.0 (0.2)	3.4 (0.1)	1.0	0.6	1.6
31	O	5		*m*-amidino	7.6 (0.6)	7.6 (1.5)	2.2 (0.2)	0.8	0.4	1.8
32	O	5		imidazolino	10.5 (0.7)	22.1 (0.6)	4.8 (0.6)	2.2	0.9	2.5
1	O	5		amidino	10.7 (0.6)	22.9 (0.7)	3.2 (0.5)	2.3	0.6	3.8
34	O	5	Cl	amidino	10.5 (0.4)	24.3 (0.3)	4.6 (0.5)	2.5	0.9	2.8
35	O	5	NH_2	amidino	10.8 (0.9)	20.7 (0.3)	3.2 (0.4)	2.1	0.6	3.5
36	O	5	NO_2	amidino	9.7 (1.2)	21.6 (1.7)	3.2 (0.2)	2.2	0.6	3.6
37	O	5	OMe	imidazolino	10.4 (1.5)	22.4 (0.3)	4.6 (0.2)	2.3	0.9	2.6
38	O	5	OMe	amidino	12.0 (0.7)	27.2 (0.1)	2.7 (0.1)	2.7	0.5	5.4
39	NH	5		amidino	11.3 (0.2)	20.7 (0.3)	4.4 (0.2)	2.1	0.8	2.5
40	NH	5	NH_2	amidino	11.0 (0.1)	20.9 (0.7)	3.3 (0.4)	2.1	0.6	3.4
41	NH	5	NO_2	amidino	12.7 (0.2)	22.1 (0.6)	6.2 (0.6)	2.2	1.2	1.9
42	O	6		amidino	9.1 (1.8)	19.0 (0.6)	2.8 (0.4)	1.9	0.5	3.6
43	O	6		*m*-amidino	7.3 (0.5)	8.1 (0.6)	2.5 (0.5)	0.8	0.5	1.7
44	O	6	NH_2	amidino	9.5 (0.7)	18.4 (2.0)	2.8 (1.1)	1.9	0.5	3.5
45	NH	6		amidino	9.1 (1.2)	12.9 (1.1)	2.9 (1.1)	1.3	0.5	2.4
46	NH	6	NH_2	amidino	8.3 (0.6)	15.0 (0.5)	3.6 (1.9)	1.5	0.7	2.2

[a] Values in parentheses are standard deviations of ΔT_m. At least one duplicate ΔT_m experiment was done for all compounds. CT refers to calf thymus DNA, AT to poly(dA)·poly(dT), and GC to poly(dGC)·poly(dGC).

Luck et al.[11] measured the DNA binding of 1, using thermal denaturation of homopolymers and natural DNA, and studied the circular dichroism of 1 bound to DNA. They also measured competition between 1 and netropsin (5) in minor-groove binding to DNA. They concluded that 1 bound to DNA and AT homopolymers in the minor groove with moderate AT base-pair specificity.

Cain[12] suggested that the activity of polycationic agents against leukemias and trypanosomes was correlated with the planarity of the molecule, the capacity to fit a radius of curvature of 20 Å, and the proper lipophilicity. Helical polynucleotides were suggested as a target for antitumor phthalanilides, 1, and analogues of 1, although experimental data with polynucleotides was presented later.[7] Using the crystal structure of 5 bound to the double-stranded DNA dodecamer GCGCAATTGCGC as a model, Goodsell and Dickerson[13] presented an isohelical analysis of the geometric parameters that could contribute to the B-DNA minor-groove binding of small molecules. They suggested that compounds with the proper isohelical curvature and chain-repeat length (4.6 Å) could bind to

(11) Luck, G.; Zimmer, C.; Schweizer, D. DNA binding studies of the nonintercalative ligand pentamidine: dA·dT basepair preference. *Stud. Biophys.* **1988**, *125*, 107–119.

(12) Cain, B. F.; Atwell, G. J.; Seelye, R. N. Potential Antitumor Agents. X. Bisquaternary Salts. *J. Med. Chem.* **1969**, *12*, 199–206.

(13) Goodsell, D.; Dickerson, R. E. Isohelical Analysis of DNA Groove-Binding Drugs. *J. Med. Chem.* **1986**, *29*, 727–733.

the minor groove of DNA. Their analysis was applied to minor-groove-binding molecules that contain polymeric repeating units. Recently, Lowe et al.[14] reported a crystal structure for 1 as the diisethionate salt. The aromatic rings and the connecting chain of 1 are coplanar. The plane of each of the amidino groups is twisted 27° from the plane of the aromatic rings. They suggest that small twist angles (15°) about the central chain of 1 shortens the interamidine distance to fit the optimal functional group spacing of the Goodsell and Dickerson[13] helical model.

This paper reports the DNA binding affinity and base pair specificity for a series of 39 analogues of 1. We determined the ΔT_m for the series with calf thymus DNA, poly(dA)·poly(dT), and (dG-dC)·poly(dG-dC) homopolymers and used this data to compare the base-sequence specificity of the bisamidines with standard minor-groove-binding compounds. In accord with literature data,[6] our viscometric titrations with calf thymus DNA indicate that the mechanism of DNA binding for the bisamidine series is not intercalation. Based upon chemical analogy and literature conclusions,[8] the DNA-binding location for the pentamidine analogues is the minor groove. To further explore this hypothesis, molecular mechanics modeling studies were done. These studies compared 1 and its analogues with crystal structures and molecular mechanics models of other classes of DNA minor-groove-binding molecules. These modeling studies confirm that the structure and conformation of 1 and its analogues is consistent with minor-groove binding.

Using reasoning analogous to that of Goodsell and Dickerson,[13] we developed a geometric parameter that can describe the fit of DNA minor-groove-binding molecules. This parameter can be applied to nonpolymeric molecules and be used to guide the design of new minor-groove-binding compounds. This parameter is the radius of curvature of the minimum-energy conformation of sets of atoms in the molecule that interact with the polynucleotide. The radius of curvature can be used to predict the DNA binding of 1 and its analogues. Analogues of 1 that cannot attain the proper radius of curvature at minimum-energy conformations show decreased binding to DNA and homopolymers in the thermal denaturation assay.

Experimental Section

Pentamidine Analogues. Syntheses of the pentamidine analogues in Table I (also see Figure 1) have been previously reported.[3,15]

Thermal Denaturation. Methods used for determining the DNA and homopolymer ΔT_ms in Table I are essentially those described by Cory.[16] Measurements were made with a Varian/Cary 2290 UV–vis spectrophotometer, with a cuvette changer holding five cuvettes. The spectrophotometer was interfaced to a microcomputer that recorded the cuvette temperature and DNA-absorbance data (at 259 nm) as the sample was heated at a rate of 18 °C/h. Calf thymus DNA was used at an initial absorbance of $0.3A_{259}$. The data collection cycle and cuvette dwell

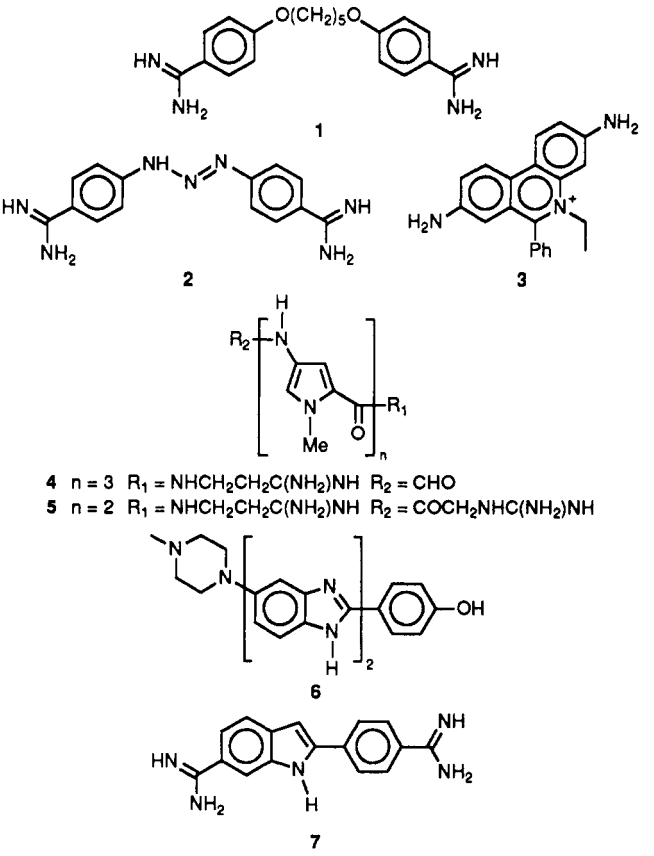

Figure 1. Structures of compounds in Table I.

times were chosen to give an interval of 0.2 °C between data points for each cuvette. The midpoint of each denaturation curve was determined after graphic selection on the computer of the starting and ending absorbance temperature for each curve of each experiment. DNA or homopolymer was run in each experiment and ΔT_ms were determined from the polynucleotide T_m for that experiment. The data in Table I represents the average of at least two determinations of the ΔT_m. Standard errors of replicate experiments are reported in Table I and control experiments with 3, a DNA intercalator, and with groove-binding molecules 2 and 4–7 are included for comparison.

Synthetic homopolymers were used to provide information on the base-pair selectivity of the compounds. To conserve materials, homopolymer experiments were done at one-half the concentration ($0.15A_{259}$) of the calf thymus DNA experiments. This did not decrease the precision of the experiments. Typical T_m values for the DNA and homopolymers under these experimental conditions are calf thymus DNA = 56.6 ± 0.8 °C, poly(dA)·poly(dT) = 40.9 ± 0.5 °C, poly(dG-dC)·poly(dG-dC) = 83.2 ± 1.2 °C.

DNA. Calf thymus DNA and homopolymers for the T_m and linear viscosity experiments were prepared by the method of Cory et al.[16] Calf thymus DNA was purchased from Worthington Biochemical Corp. Homopolymer poly(dA)·poly(dT) was purchased from Boehringer Mannheim, and poly(dG-dC)·poly(dG-dC) was purchased from Pharmacia LKB Biotechnology Inc. Ethidium bromide (3) and distamycin A (4) were purchased from Sigma Chemical Co. Netropsin hydrochloride (5) was purchased from Serva Feinbiochemica. Hoechst 33258 (6) and DAPI (7) were purchased from Aldrich Chemical Co.

Viscometric Titrations. Titrations with sonicated calf thymus DNA (Figure 2) were carried out on selected compounds using the method of Cohen and Eisenberg[17] as modified by Cory et al.[16] Time readings were accumulated by a Macintosh computer interfaced to a Wescan (Wescan Instruments, Santa Clara, CA)

(14) Lowe, P. R.; Sansom, C. E.; Schwalbe, C. H.; Stevens, M. F. G. Crystal Structure and Molecular Modelling of the Antimicrobial Drug Pentamidine. *Chem. Commun.* **1989**, *16*, 1164–1165.
(15) Jones, S. K.; Hall, J. E.; Allen, M. A.; Morrison, S. D.; Ohemeng, K. A.; Reddy, V. V.; Geratz, J. D.; Tidwell, R. R. Novel Pentamidine Analogs in the Treatment of Experimental Pneumocystic carinii Pneumonia. *Antimicrob. Agents Chemother.* **1990**, *34*, 1026–1030.
(16) Cory, M.; McKee, D. D.; Kagan, J.; Henry, D. W.; Miller, J. A. Design, Synthesis, and DNA Binding Properties of Bifunctional Intercalators. Comparison of Polymethylene and Diphenyl Ether Chains Connecting Phenanthridine. *J. Am. Chem. Soc.* **1985**, *107*, 2528–2536.
(17) Cohen, G.; Eisenberg, H. Viscosity and Sedimentation Study of Sonicated DNA-Proflavine Complexes. *Biopolymers* **1969**, *8*, 45–55.

Table II. Radii of Curvature for Standard DNA Minor-Groove-Binding Molecules and Analogues of 1

no.	radius of curvature, Å	name	comments[b]
	19	DNA	standard geometry for AAAA double-stranded B-DNA using position of the 2-amino group of adenine
	60	DNA	AATT region from dodecamer crystal structure as above
1	77		FMNR using CA and O
2	14	berenil	FMNR using CA ring C
4	15	distamycin A	crystal structure in dodecamer CA and guanidino C and three pyrrole ring atoms
	40		FMNR using same atoms
5	15	netropsin	crystal structure in dodecamer CA and guanidino C along with two pyrrole ring atoms
6	20	Hoechst 33258	crystal structure in dodecamer; the atoms used were those that connected the ring systems
7	1400	DAPI	(4',6-diamidino-2-phenylindole) Uses CA and indole C atoms
8	703		
12	14		
13	143		180° twist about C–O–C bond from lowest energy starting point
	29		180° twist about both C–O–C bonds
	5.9		lowest energy conformer
22	291153		
23	180000		lowest energy conformer
	2800		180° twist about one C–O–C bond from above starting point
41	15		pentamidine analogue with NH and amino substituent CA ring C
42	68000		FMNR using CA and O

[a] Molecular models were computed with MacroModel version 2.5 using the AMBER force field and FMNR minimization. [b] CA refers to the carbon atom in the amidine. Ring C refers to the carbon to which the amidino group is attached. O refers to the heteroatom opposite the amidine in the pentamidine series. FMNR is full-matrix Newton–Rafson molecular mechanics minimizer used with the AMBER force field as implemented in version 2.5 of MacroModel.

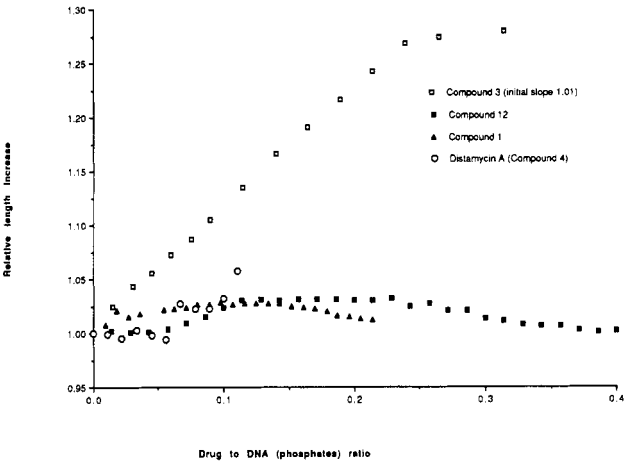

Figure 2. Viscometric titrations of calf thymus DNA with ethidium bromide and various groove-binding molecules.

viscosity timer that timed the liquid flow in a Cannon-Ubbelohde viscometer. Flow times were accumulated until two times were within 0.2 s. A custom-built interface to the Macintosh automated the drug delivery to the viscometer and the fluid handling necessary to operate the viscometer.

Molecular Modeling. Molecular mechanics models of 1 and its analogues in Table II were generated using version 2.5 of MacroModel[18] and the AMBER force field option as implemented in the MacroModel program on a DEC/VAX computer. No changes to the force field geometric or electronic parameters were necessary for these calculations. Parameters are available for the amidino group as a substructure of the guanidino group in arginine. The remaining atom types are commonly occurring fragments for which parameters were available in the MacroModel implementation of the AMBER force field. An appendix lists the parameters and resulting forces for 1 during a single-point energy calculation at the minimum corresponding to the crystal structure. Partial atomic charges for the atoms were calculated by the MacroModel program. Explicit hydrogen atoms were included in all calculations. Since essentially planar models were desired for 1 and its analogues, the initial minimizations included geometric constraints. This was designed to give models consistent with the crystal structure of 1. Using a two-dimensional sketch as a starting point, geometric constraints were set that forced the molecule into an extended conformation. A limited number of iterations, typically 100, using the block diagonal Newton–Rafeson (BDNR) minimization technique were performed to extend the molecule.

After this partial minimization of the constrained molecule, the constraints were removed, and each model was fully minimized using BDNR minimization. Each minimized conformation was tested for full minimization using the full-matrix Newton–Rafeson (FMNR) minimizer. Fully extended models for 1 and its analogues resulted from this procedure. The minimized C–O–C bond angle was 118.0°. This compares to 117.8° found in the crystal structure of 1.[14] The resulting all-atom model has a 0° torsion angle between the amidino group and the benzene ring. The torsion angle of the molecular mechanics minimum for the imidazoline system of compounds **15** and **21** was also 0°. Adding a methyl group to one of the nitrogen atoms of the imidazoline system gave a minimum-energy conformer with a torsion angle of 15.3°. A 30 ± 12° torsion is seen in crystal structures of free benzamidines, and a 27° torsion was found in the published structure of 1.[14]

Crystal structures of the minor-groove-binding molecules distamycin A (**4**) (Brookhaven file[19] 2DND),[20] netropsin (**5**) (6BNA),[21] and Hoechst (**6**) 33258 (1DNH)[22] were taken from the drug–DNA complexes as reported in the Brookhaven Crystallographic Database. The crystal coordinate files were loaded into MacroModel and fully minimized without the nucleic acid fragment to give structures that were generally planar. The procedures discussed above, without constraints, were used for these calcu-

(18) Mohamadi, F.; Richards, N. G. J.; Guida, W. C.; Liskamp, R.; Lipton, M.; Caufield, C.; Chang, G.; Hendrickson, T.; Still, W. C. MacroModel—An Integrated Software System for Modeling Organic and Bioorganic Molecules using Molecular Mechanics. *J. Comput. Chem.* **1990**, *11*, 440–467.

(19) Bernstein, F. C.; Koetzle, T. F.; Williams, G. J. B.; Meyer, E. F.; Brice, M. D.; Rogers, J. R.; Kennard, O.; Shimanouchi, T.; Tasumi, M. The Protein Data Bank: A Computer-based Archival File for Macromolecular Structure. *J. Mol. Biol.* **1977**, *112*, 535–542.

(20) Coll, M.; Frederick, C. A.; Wang, H.-J.; Rich, A. A Bifurcated Hydrogen-bonded Conformation in the d(AT) Base Pairs of the DNA Dodecamer d(CTCAAATTTGCG) and its Complex with Distamycin. *Proc. Natl. Acad. Sci. U.S.A.* **1987**, *84*, 8385–8389.

(21) Kopka, M. L.; Yoon, C.; Goodsell, D.; Pjura, P.; Dickerson, R. E. Binding of an Antitumor Drug to DNA. Netropsin and CGCGAATTBrCGCG. *J. Mol. Biol.* **1985**, *183*, 553–563.

(22) Teng, M.-K.; Usman, N.; Frederick, C. A.; Wang, H.-J. The Molecular Structure of the Complex of Hoechst 33258 and the DNA Dodecamer d(CGCGAATTCGCG). *Nucleic Acids Res.* **1988**, *16*, 2671–2690.

lations. Both the crystal structure and the minimum energy, planar model were used to compute the radius of curvature data found in Table II. It was not necessary to add force-field parameters to MacroModel for the minimizations of the crystal structures of **4–6**. The radii of curvature for the minor groove of one model structure and one crystal structure of B-DNA were also calculated. MacroModel provides a B-DNA template in the AMBER force field implementation, with planar Watson–Crick base pairs, 10 base pairs per turn, and base pairs perpendicular to the helix axis with 3.4-Å separation. A $d(AT)_4$ oligonucleotide was generated using the standard template. The nitrogen atom of the 2-amino groups of the adenine in the minor groove were used for the radius of curvature measurements on the DNA model. The same groups were used for the measurement of the central AATT section of the X-ray structure (6BNA)[21] of **5**.

Computation of the radius of curvature of compound **1** and its analogues, presented in Table II, was done by selection of the atoms shown in Figure 4. A Microsoft Excel spreadsheet was used to compute the radius of the sphere that was specified by the x, y, z coordinates of the four selected atoms. Atoms on the "inner" face of the molecule were chosen for the curvature computations on the minimized models of the standard compounds. The method of computation is derived from the general formula for a sphere with center (a,b,c) and radius r:

$$(x - a)^2 + (y - b)^2 + (z - c)^2 = r^2$$

This equation is rearranged and rewritten in vector notation as

$$(-2\mathbf{x},-2\mathbf{y},-2\mathbf{z},1)\cdot(\mathbf{a},\mathbf{b},\mathbf{c},\mathbf{k}) = -\mathbf{x}^2 - \mathbf{y}^2 - \mathbf{z}^2$$

where

$$\mathbf{k} = \mathbf{a}^2 + \mathbf{b}^2 + \mathbf{c}^2 - \mathbf{r}^2$$

When the above step is repeated for each of four points, there are four linear equations in four unknowns. Through matrix techniques, **a**, **b**, **c**, and **k** can be found. Then **r** is computed from the formula for **k** above. Coordinate files in MacroModel ASCII format for all of the structures in Table II are available from the authors upon request.

Results and Discussion

Increases in DNA or homopolymer thermal denaturation temperature are reported for sonicated calf thymus DNA and homopolymers poly(dA)·poly(dT) and poly(dG-dC)·poly(dG-dC) as ΔT_m values (Table I) representing the difference in the denaturation temperature midpoint for the drug–polynucleotide complex as compared to the polynucleotide alone in the same experiment. Since calf thymus DNA is heterogeneous in base sequence and about 50% GC, the ΔT_m, with calf thymus DNA, characterizes the strength of the interaction with heterogeneous base sequences. Although, the ΔT_m was not directly converted to a binding constant, it represents an averaging of the binding constant over the multiple sequences of the heterogeneous sites of the DNA. As an approximate benchmark, ethidium bromide (**3**), with a ΔT_m of 12.4 °C in this buffer system (Table I), showed a binding constant of $1.6 \cdot 10^6$ [23] with calf thymus DNA, when determined by ultraviolet spectrophotometric titration and Scatchard analysis of the binding data. The ΔT_m of 10.7 °C shown by **1** (similar to the ΔT_m of **3**) indicates that the binding constant of **1** should be in the 10^6 range in this buffer.

The homopolymer ΔT_m data reported in Table I characterizes the affinity of the compounds for a more limited set of DNA-binding sites and can give an indication of base-sequence specificity for DNA-binding molecules. However, because of differences in the homopolymer T_m, direct comparison of the magnitude of the ΔT_m values for

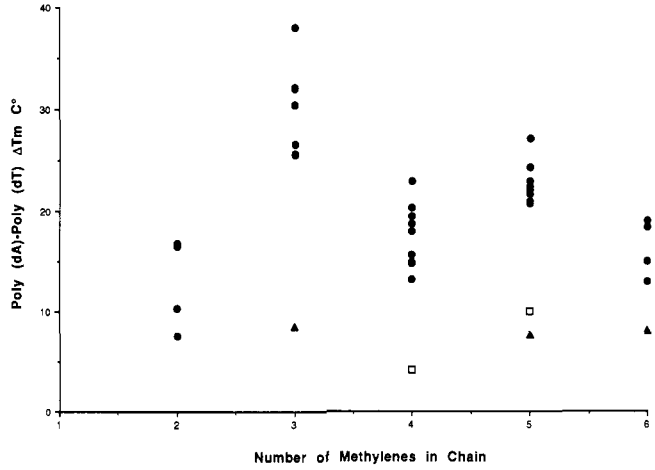

Figure 3. Relationship between poly(dA)·poly(dT) ΔT_m and the number of methylenes in the connecting chain: ●, polymethylene chains; ▲, meta-amidino; □, *N*-methyl-2-imidazolinyl system.

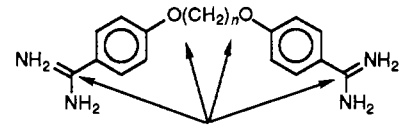

Figure 4. Points used for radius of curvature calculation.

calf thymus DNA and the homopolymers poly(dA)·poly(dT) and (dG-dC)·poly(dG-dC) cannot be made. We chose instead to normalize the ΔT_m by comparison with ethidium bromide (**3**), a compound that shows little base-pair specificity.[24] Table I shows the normalized ΔT_m values for the homopolymers and the AT/GC ratios of the normalized ΔT_ms for the analogues of **1** in comparison with values for a series of standard DNA-binding compounds showing various AT base-pair specificity. Compounds **4–6** showed high AT base-pair specificity. Although the magnitude of the AT to GC ratio for **4** was lower than that previously found,[8] compound **4** did show a substantial AT preference. Compound **7**, shown to bind to the same site in the double-stranded dodecamer CGCGAATTCGCG sequence as **4**,[25] can also act as an intercalator in GC sequences[26] and showed moderate AT specificity by our normalization method. Most of the analogues of **1** showed modest (<3) AT to GC ratios. The exceptions are compound **16**, with a ratio of 6, and compound **27**, with a ratio of 11. Both of these compounds have MeO groups on the benzamidine moiety that may contribute to base-pair specificity, although no significant relationship between aromatic ring substituent and base-pair specificity was apparent. The moderate AT base pair specificity shown by the bisamidines could be the result of the highly electropositive bisamidines binding preferentially to the most electronegative region of the DNA, the AT base pairs in the minor groove. Groove-binding compounds such as **4** and **5** showed the high preference for AT regions on the basis

(23) Cory, M.; Bair, K. W.; Fairley, T.; McKee, D. D., unpublished results.

(24) Williams, R. E.; Seligy, V. L. The Interaction of Ethidium Bromide with Synthetic Polydeoxyribonucleic Acids. Effect of Base Composition and Sequence on the Induced Circular Dichroism Spectra. *Can. J. Biochem.* **1974**, *52*, 281–287.

(25) Larsen, T. A.; Goodsell, D. S.; Cascio, D.; Grzeskowiak, K.; Dickerson, R. E. The Structure of DAPI Bound to DNA. *J. Biomol. Struct. Dyn.* **1989**, *7*, 477–491.

(26) Wilson, W. D.; Tanious, F. A.; Barton, H. J.; Strekowski, L.; Boykin, D. W. Binding of 4',6-Diamidino-2-phenylindole (DAPI) to GC and Mixed Sequences in DNA: Intercalation of a Classical Groove-Binding Molecule. *J. Am. Chem. Soc.* **1989**, *111*, 5008–5010.

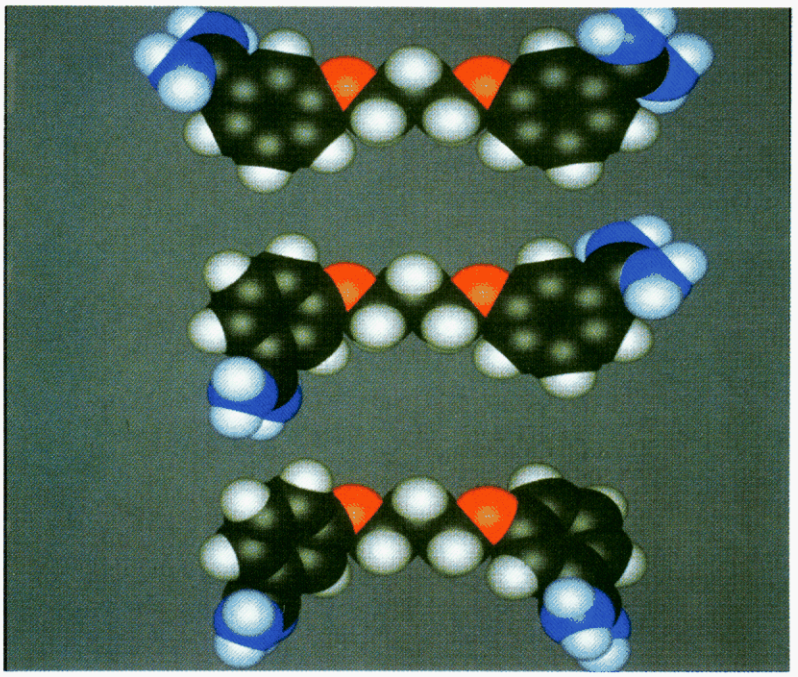

Figure 5. CPK representations of the molecular mechanics models of compound **13**: conformer A (top), B (middle), and C (bottom).

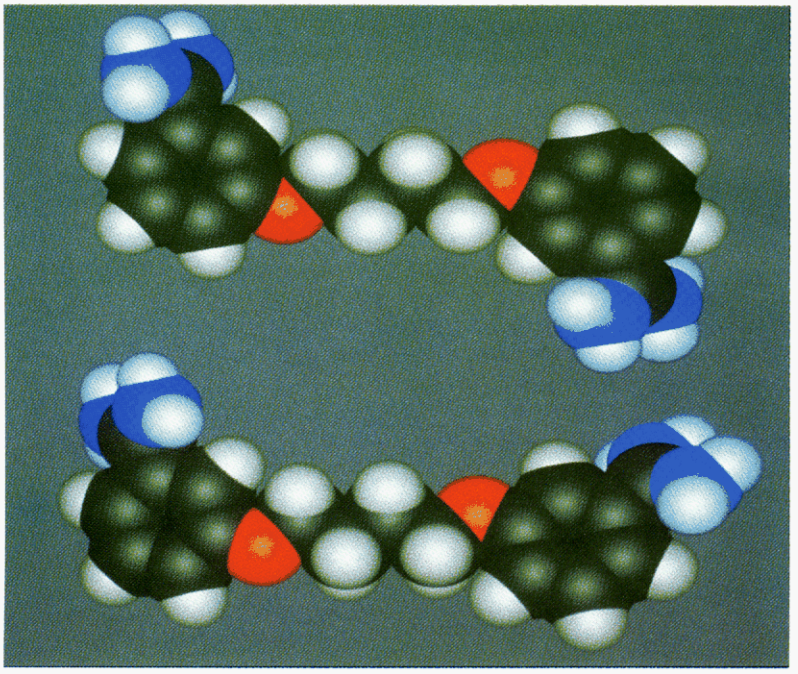

Figure 6. Two conformers of compound **23**.

of steric hindrance to GC binding. The much more flexible analogues of **1** probably interact with electrostatic forces rather than by steric forces.

Increases in DNA viscosity as shown during viscometric titrations with calf thymus DNA can be a diagnostic indicator of intercalative DNA binding.[16] Viscometric titrations were done with standard DNA-binding compounds **3** and **4** as control compounds, compound **1**, and selected analogues of **1**. If **1** or its analogues were intercalating into the DNA, it should be possible to detect insertion of the aromatic benzamidine ring system between the base pairs. This insertion would cause a substantial viscosity increase, corresponding to a DNA chain length increase. Monointercalating compounds, in this experiment, were characterized by an initial titration slope near unity. Nonintercalating compounds showed slopes close to zero. The results of some of these experiments are plotted in Figure 2. Compound **3** is a monointercalator, it showed an initial slope (Figure 2) of 1.01. Nearest-neighbor-excluded binding, a characteristic of intercalators, is shown by saturation of the available DNA-binding sites. This saturation is seen as a leveling of the viscosity slope at a compound to base ratio of 0.25. Compound **4**, a minor-groove-binding molecule showed an insignificant slope in the initial part of the titration (Figure 2). Compound **1** and **12** had very low initial slopes at the start of the titration, and a zero slope after that. These viscometric titrations indicate that **1** and its analogues bind to DNA

by a nonintercalative mechanism. This data combined with the spectral data of Luck et al.[11] suggests that 1 and its analogues bind to B-DNA in the minor groove.

Figure 3 is a plot of the ΔT_m of the homopolymer poly(dA)·poly(dT) (data from Table I) versus the number of methylene carbon atoms in the connecting linker for the analogues of 1. Compounds with three and five methylenes showed higher AT site affinity on average, while lower affinity was demonstrated for the compounds with two, four, and six methylenes. Plotting the data for this series in this manner suggests that poly(dA)·poly(dT) affinity is governed by the shape of the molecules. Similar alternating high and low ΔT_m results were obtained with the calf thymus and poly(dG-dC)·poly(dG-dC) (Table I), although the magnitude of the differences is smaller.

Specifically indicated in Figure 3 are two sets of compounds that do not fit into the alternating pattern. These compounds showed weak binding to poly(dA)·poly(dT) sites compared to other compounds with the same chain length. The two *N*-methylimidazolines (**20, 30**) show low affinity for poly(dA)·poly(dT) sites when compared with compounds that have a corresponding number of methylene groups. The set of four compounds in which the amidino group is meta (**13, 23, 31, 43**) to the linking bridge also showed low affinity for poly(dA)·poly(dT) regardless of the number of methylenes in the connecting chain.

Molecular mechanics studies were used to obtain minimum-energy conformations of the amidino, imidazolino, and *N*-methylimidazolino groups when substituted on a benzene ring. The model studies gave a minimum for benzamidine that is planar. Crystal structures of benzamidine[27] and 1[14] alone suggest that a small dihedral angle 30° is more realistic in aqueous solution. When it was bound to a macromolecule, benzamidine showed a 0° dihedral angle. For benzimidazoline the minimum was also 0°. There was less hindrance to planarity for the benzimidazoline system in comparison to benzamidine. The imidazoline ring directs the hydrogen atoms away from the ortho hydrogen atoms on the benzene ring. However, the minimum energy for the *N*-methylimidazoline ring was 15°. This torsion was due to steric interaction between the hydrogen atoms of the *N*-methyl group and the ortho hydrogen atoms of the aromatic ring. These modeling results suggest that the lack of planarity, or the high-energy cost of attaining planarity for the *N*-methylimidazolino group, prevents optimal binding in the minor groove of DNA. Since crystal structures of benzamidines suggest that the torsion angle should be larger than 0°, it also might be expected that the *N*-methylimidazolino torsion angle would be substantially larger than 15°. No crystal data is available on this point.

In comparison to the amidino group, the imidazolino group showed no consistent differences in binding to DNA or the homopolymers (compare compounds **15** to **16**, **21** to **22**, and **1** to **32**). Cyclization of the amidino group into the imidazolino group decreased the number of hydrogen atoms available for hydrogen-bonding interaction with the DNA and lowered the pK_a of the amidino functional group. However, the change in pK_a is probably unimportant since the imidazolines would still interact with DNA as cations. The bulk of the ethylene bridge does not inhibit groove binding since it can lie parallel to the walls of the groove in the minimum energy, dihedral angle of 0°, conformation.

The two 1-methyl-2-imidazolines (**20** and **30**) showed weak binding to the polynucleotides in comparison to similar imidazolines (compare **20** to **21** and **30** to **32**). Twisting the 1-methyl-2-imidazolinyl group out of plane did not entirely prevent compounds **20** and **30** from binding to DNA but lowered their affinity considerably. These compounds probably bind with the methyl group pointing away from the bases in the floor of the groove and still maintain its positive charge.

Goodsell and Dickerson[13] suggested a method for computing the helix-repeat length (4.6 Å) necessary for interaction with the functional groups in adjacent base pairs on the floor of the minor groove and calculated the helix-repeat spacing for various heterocyclic monomeric units that could be incorporated into polymers analogous to **4** and **5**. This series of compounds with varying chain lengths does not conform to this structural unit repeating motif. The method proposed by Lowe[14] for twisting 1 to fit the 4.6-Å repeat length also does not apply to a series of molecules containing different chain lengths. We therefore tried to describe the interaction of 1 and its analogues with a metric that was different from the helix-repeat length.

We have found that the radius of curvature of the atoms on the curved inner face of the molecule is an effective measure of the optimal shape for the minor-groove-binding molecules. Table II contains the radius of curvature of two different DNA structures. One DNA structure is a standardized B-DNA model found in the MacroModel program containing idealized bond lengths and angles. The second radius of curvature is from the AATT region of the X-ray crystal structure of **5** complexed with a double-stranded dodecamer (file 6BNA).[21] Also in Table II is the radius of curvature measurement from X-ray crystal structures and molecular mechanics models of a series of known minor-groove-binding molecules. We also computed the radius of curvature for compound 1 and some of its analogues from molecular mechanics models.

The crystal structures of the minor-groove-binding molecules **4** and **5** show a radius of curvature of 15 Å (Table II) when bound to the minor groove of DNA. This radius matches closely the DNA minor-groove radius of 19 Å and is similar to the 40-Å radius shown by the fully planar molecular mechanics minimized molecules. Small, 4°–15°, dihedral angle changes are necessary to convert the planar minimized model to the bound crystal structure. The X-ray crystal structure of netropsin alone shows a fully extended conformation with a 25° dihedral angle between pyrrole rings.[28]

For the bisamidine series, the data in Table II shows that the compounds with three and five methylenes in the chain have a radius of curvature similar to DNA (compound 1 has a radius of curvature of 77 Å and compound **12** has a radius of 14 Å). On the other hand, the compounds with two (**8**, radius of curvature = 703 Å), four (**22**, radius of curvature = 291 000 Å), or six methylenes have extremely large radii of curvature, consistent with the linear shape of the molecules. In the linear molecules, the magnitude of the radius of curvature is very sensitive to the final molecular mechanics model. Small motions of the atoms can cause large changes in the magnitude of the radius of curvature since a perfectly linear molecule would give an infinite radius. However, for the larger linear molecules, the DNA affinity is not sensitive to large radius of curvature changes since large changes in radius of curvature can represent minor conformational differences.

(27) Bode, W.; Schwager, P. The Refined Crystal Structure of Bovine Beta-Trypsin at 1.8 Å Resolution. Crystallographic Refinement, Calcium Binding Site, Benzamidine Binding Site and Active Site at pH 7.0. *J. Mol. Biol.* **1975**, *98*, 693–717.

(28) Berman, H. M.; Neidle, S.; Zimmer, C.; Thrum, H. Netropsin, a DNA-binding oligopeptide. Structural and binding studies. *Biochim. Biophys. Acta* **1979**, *561*, 124–131.

A molecule with a radius of curvature, less than that of the minor groove, has a much lower DNA affinity. In the highly curved molecules greater conformational changes are needed in the molecule to open the radius of curvature to that of the DNA minor groove. These large conformational changes have a higher energy and therefore lower the DNA affinity of the compound.

Low polynucleotide affinity was seen with the meta-substituted compounds (compare **12** with **13**, **1** with **31**, and **42** with **43**); this was most distinct with the AT homopolymer. This low DNA and homopolymer affinity of the meta-substituted compounds can also be rationalized by their shape. In this situation the meta compounds do not have low-energy conformers consistent with DNA minor-groove binding. Study of the conformers in the meta cases is complicated by rotational conformers of the aromatic rings, therefore more than one meta conformer must be considered. Analysis of the molecular models of **13** shows that there are three planar relatively low-energy conformations of the molecule. Molecular models of these three conformations are shown in Figure 5. The data in Table II show that none of the conformations have a radius of curvature close to that required for the minor groove of DNA. Conformer **A** in Figure 5 has the lowest molecular mechanics energy and also has a radius of curvature that is much too large for facile interaction with the minor groove. Conformer **B** (middle structure) has a radius of curvature close to ideal for interaction with the minor groove, but in this conformer the amidino groups are on opposite sides of the aromatic rings and only one of the amidino groups at a time can interact with the DNA. Conformer **C** in Figure 5 has both of the amidino groups on the same side of the benzene rings and is higher in energy than conformer **A** or **B**. Conformer **C** has a radius of curvature that is too small to allow full interaction with DNA. Table II contains two radius of curvature measurements for the two conformers of compound **23** containing a four methylene linking unit and meta-substituted amidine groups. Space-filling molecular mechanics models of these two conformers are shown in Figure 6. Neither of these conformers has the proper radius of curvature to be an effective minor-groove-binding compound.

In conclusion, our studies show that the strength of DNA or homopolymer polynucleotide minor-groove-binding, as described by a thermal denaturation assay, of a large series of pentamidine (**1**) analogues can be described by the conformation of the molecules. The radius of curvature of molecular mechanics models can act as a descriptor of the strength of DNA groove binding. This measurement can be used to predict the minor-groove-binding properties of hypothetical new anti-PCP compounds. This effect is seen as a relative strengthening and weakening of the DNA-binding interaction. Although all of the compounds in this series did bind to DNA and homopolymers, all of the compounds also show some activity, within the limitations of toxicity, in the in vivo *P. carinii* assay.[3]

Acknowledgment. We thank Susan Pulley and Carrie McClung for assistance with the DNA binding measurements, Daniel Cory for assistance with the radius of curvature measurements, and Lisa St. John for the automation of the viscosity measurements. These studies were funded in part by Public Health Service Contract N01-AI-7264.

2-[(2-Pyridylmethyl)sulfinyl]-1*H*-thieno[3,4-*d*]imidazoles. A Novel Class of Gastric H^+/K^+-ATPase Inhibitors

Klaus Weidmann,* Andreas W. Herling, Hans-Jochen Lang, Karl-Heinz Scheunemann, Robert Rippel, Hildegard Nimmesgern, Thomas Scholl, Martin Bickel, and Heinz Metzger

Hoechst AG, Pharma Research, P.O. Box 80 03 20, 6230 Frankfurt 80, Germany. *Received March 5, 1990*

2-[(2-Pyridylmethyl)sulfinyl]thienoimidazoles were synthesized and investigated as potential inhibitors of gastric H^+/K^+-ATPase. The [3,4-*d*] isomers of the two possible thienoimidazole series were found to be potent inhibitors of gastric acid secretion in vitro and in vivo. Structure–activity relationships indicate that especially lipophilic alkoxy, benzyloxy, and phenoxy substituents with additional electron-demanding properties in the 4-position of the pyridine moiety combined with an unsubstituted thieno[3,4-*d*]imidazole lead to highly active compounds with a favorable chemical stability. Various substitution patterns in the thieno[3,4-*d*]imidazole moiety result in lower biological activity. The heptafluorobutyloxy derivative saviprazole (HOE 731, **5d**) was selected for further development and is currently undergoing clinical evaluation. Comprehensive pharmacological studies indicate a pharmacodynamic profile different to omeprazole, the first H^+/K^+-ATPase blocker introduced on the market.

Introduction

Inhibition of gastric acid secretion has been proven to be a powerful therapeutic principle in the treatment of gastric and duodenal ulcer disease.[1] Gastric acid secretion is regulated by interaction of basolateral parietal cell receptors with their physiological stimulants gastrin, acetylcholine, and histamine.[2] Anticholinergics and especially H_2-receptor antagonists have therefore become antisecretory agents of major importance.

2-[(2-Pyridylmethyl)sulfinyl]benzimidazoles like omeprazole represent a new class of effective gastric acid secretion inhibitors.[3] Their antisecretory activity has been ascribed to a highly specific inhibitory action on the gastric proton pump, the H^+/K^+-ATPase,[4] which is responsible for the transport of gastric acid into the lumen of the

(1) Soll, A. H.; Isenberg, J. I. In *Duodenal Ulcer Diseases in Gastrointestinal Disease*; Sleisenger, M. H., Fordtran, J. S., Eds.; Saunders: Philadelphia, 1983; pp 625–672.

(2) Sachs, G. The Parietal Cell as a Therapeutic Target. *Scand. J. Gastroenterol. Suppl.* **1986**, *21* (Suppl. 118), 1–10.

(3) Fellenius, E.; Berglindh, T.; Sachs, G.; Olbe, L.; Elander, B.; Sjöstrand, S.-E.; Wallmark, B. Substituted Benzimidazoles Inhibit Gastric Acid Secretion by Blocking (H^+/K^+)-ATPase. *Nature* **1981**, *290*, 159–161.

(4) (a) Ganser, A. L.; Forte, J. G. K^+-Stimulated ATPase in Purified Microsomes of Bullfrog Oxyntic Cells. *Biochim. Biophys. Acta* **1973**, *307*, 169–180. (b) Sachs, G.; Chang, H. H.; Rabon, E.; Schackmann, R.; Lewin, M.; Saccomani, G. A Non-Electrogenic H^+-pump in Plasma Membranes of Hog Stomach. *J. Biol. Chem.* **1976**, *251*, 7690–7698. (c) Wallmark, B.; Larsson, H.; Humble, L. The Relationship Between Gastric Acid Secretion and Gastric H^+/K^+-ATPase Activity. *J. Biol. Chem.* **1985**, *260*, 13861–13684.

0022-2623/92/1835-0438$03.00/0